IEEJ Journal of Industry Applications
Vol.7 No.2 pp.158–165 DOI: 10.1541/ieejjia.7.158

Paper

Translation and Inclination Control for Intelligent Tension Pole Based on Mode Decoupling Method

Ryo Hanaoka* Non-member, Takahiro Nozaki* Member
Toshiyuki Murakami* Fellow

(Manuscript received Nov. 30, 2016, revised July 16, 2017)

An aging society is a serious problem in many developed countries. Due to this issue, there has been a significant increase in the demand for assist devices that can support human motion. This paper proposes a novel assist device, Intelligent Tension Pole (ITP), to assist in indoor activities of daily living (ADL), and it is expected to provide support for achieving self-reliance, space saving, and stability. The structure and control system of this assist device are presented. This novel assist device is based on a movable handrail, and therefore wheels are added to the lower and upper ends of the tension pole. In addition, a ball screw, which enables the ITP to move while stretching to the floor and ceiling at any time using force control, is added. In order to improve user comfort and reduce the risk of falling down of the ITP, translation and inclination controls of the ITP are applied to the wheel control. These controls are controlled independently by the mode decoupling method. Experiments are conducted to verify the effectiveness of the proposed device and its control system.

Keywords: tension pole, handrail, motion assistance, mode decoupling, inertial measurement unit (IMU)

1. Introduction

In recent years, an aging society and fewer children have become serious problems in many developed countries. While the number of the elderly people who need care are increasing, the number of the care workers are reducing, and there are not enough welfare facilities for the needs. Moreover, the rate of elderly people who live alone is in a tendency toward increasing. So, the assist device for elderly people to live by themselves is demanded. Especially, walking, standing up and sitting down are the important movements to live by themselves. These movements are called as activities of daily living (ADL) and defined as indispensable basic movements in living. The activity area largely changes whether they can do these movements by themselves or not. Therefore, it is important for their quality of lives (QOL) to maintain the ability for these movements. To address this issue, the motion assist device which promotes elderly people to walk, stand up and sit down by themselves has been attracting attention.

There are many kinds of walking assist device based on the walker [(1)–(3)]. While they have stable structure by more than four ground points and can support the elderly's upper body while walking, it is often difficult to be used in the narrow space like the corridor because of their wide body. Also, there are some standing up or sitting down assist devices which are constructed with the chair part and upper body supporting part [(4)(5)]. However, many of these devices do not have the moving mechanism. Thus, while standing up from the bed, walking around and sitting down on the toilet are the important series of movements in life, there are few devices which can assist all of these movements without inconvenience. In late years, wearable assist devices have been studied a lot [(6)(7)]. These devices have high mobility and can be used under various environment. However, they can not support the balance of the body sufficiently, so the users must be able to keep their own balance by themselves.

As a novel walking, standing up and sitting down assist device, this paper presents the Intelligent Tension Pole (ITP), which is expected to provide support for achieving self-reliance, space saving, and stability. The ITP is based on the tension pole used for supporting standing up and sitting down mainly. The tension pole has high stability by multiple ground points and does not need space very much. The problems of the conventional tension pole include that the activity area is limited only at setting point and multiple tension poles are needed to support walking. To solve these problems, the structure and control system of the ITP are proposed. The main contributions of this paper are the development of the ITP structure because there has been no walking, standing up and sitting down assist device based on the tension pole, and the development of the control system which the user comfort and stability are improved.

In terms of the structure, the moving mechanism by wheels attached on the upper and lower ends of the tension pole, additionally the expansion and contraction mechanism by the ball screw are applied so that the ITP can move while stretching to the floor and ceiling at any time as the movable handrail. Thereby, the ITP can assist walking, standing up and sitting down with one device. Also in terms of the control, the force control is applied to the ball screw control to

* Toshiyuki Murakami Labo. System Design Engineering Department Keio University
3-14-1, Hiyoshi, Kohoku-ku, Yokohama 223-8522, Japan

prevent the slip of the ground points of the ITP [8]. In addition, the translation control and inclination control are applied to the wheel control in order to improve the user comfort and reduce the risk of falling down of the ITP. Then, these translation and inclination control are controlled independently by the mode decoupling method. In this paper, an Inertial Measurement Unit (IMU) which contains a 3-D accelerometer and a 3-D angular rate sensor is used to detect the human motion and to use the human motion data for the control in real time.

The paper is organized as follows. Section 2 gives a description of the ITP, and the modeling is explained in section 3. In section 4, the walking motion estimation with an IMU is explained. Section 5 explains the control system, and experiments are carried out to verify the proposed controller in section 6. Finally, this paper is concluded in Section 7.

2. System Description

In this section, the system description of proposed assist device is explained. The ITP is constructed with two parts; wheel part and ball screw part. The human motion is detected by an IMU. The structure and the use example of the ITP are shown in Fig. 1(a) and Fig. 1(b).

2.1 Wheel Part The two-wheel and one-wheel are added to the lower and upper ends of the tension pole. The space saving is achieved by reducing the number of the lower wheel and making the structure smaller. For this reason, users can bring their body close to the device and walk stably and safely when the users walk while catching the ITP. Furthermore, thanks to the two-wheel structure of the lower end, the ITP has the passive joint in the pitch direction. It enables to change the inclination of the ITP and keep the desired pitch angle under the slope or step environment.

2.2 Ball Screw Part The ball screw is applied to the ITP in order to achieve the expansion and contraction to the vertical direction. By adjusting the length depending on the inclination of the ITP, it can stretch to the floor and ceiling at any time. In addition, the ball screw enables to control the tension force between the floor and ceiling.

2.3 IMU An IMU is attached on the one side foot to detect the user's foot motion. In this research, the horizontal foot acceleration with respect to the ground is measured by the acceleration and angular velocity data received from the IMU.

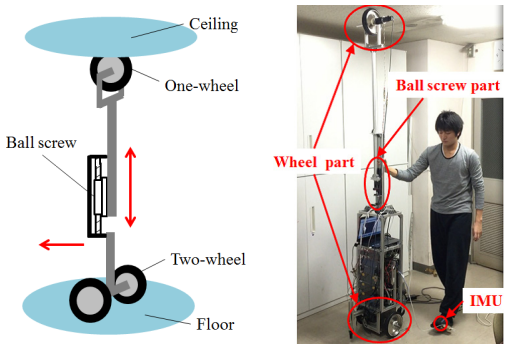

(a) Structure (b) Use example

Fig. 1. Structure and use example of ITP

3. Modeling

In this section, the modeling of the ITP is described. The top view and side view of the ITP are shown in Fig. 2(a) and Fig. 2(b). In addition, the modeling of the ball screw is shown in Fig. 3. The parameters used for the modeling are shown in Table 1.

3.1 Kinematics of ITP In the kinematics of the ITP, two assumptions are considered as below.

- The ITP does not move toward axle direction
- Wheels do not slip

From the first assumption, (1) is derived.

$$Y = 0 \cdots\cdots (1)$$

Also from the second assumption, (2) is derived.

$$\dot{d} = X = R\dot{\phi}_0 \cdots\cdots (2)$$

The variable vectors are defined as $\boldsymbol{X} = \left[d, \theta_p, L_1, \phi_1\right]^T$, $\boldsymbol{\theta} = \left[\phi_0, \theta_p, L_1, \phi_1\right]^T$. Then, the direct kinematics is expressed as (3) and the inverse kinematics is expressed as (4).

$$\dot{\boldsymbol{X}} = \boldsymbol{J}_{aco}\dot{\boldsymbol{\theta}} \cdots\cdots (3)$$
$$\dot{\boldsymbol{\theta}} = \boldsymbol{J}_{aco}^{-1}\dot{\boldsymbol{X}} \cdots\cdots (4)$$

Where, $\boldsymbol{J}_{aco}$ denotes the Jacobian matrix given as (5).

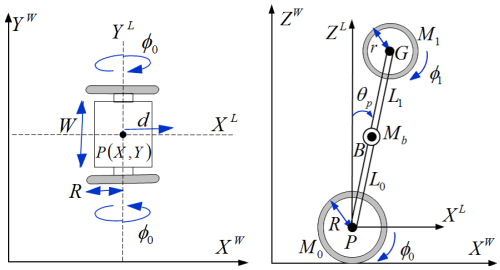

(a) Top view (b) Side view

Fig. 2. Modeling of ITP

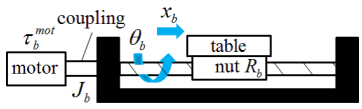

Fig. 3. Modeling of ball screw

Table 1. Parameters of ITP

Parameter	Unit	Name
$\bigcirc^W$		World coordinate
$\bigcirc^L$		Robot coordinate
X, Y	m	Position of robot in world coordinate
P		COG of lower wheels
B		COG of ball screw
G		COG of upper wheel
W	m	Tread between lower left and right wheels
d	m	Translational distance
R	m	Radius of lower wheels
r	m	Radius of upper wheel
ϕ_0	rad	Direction angle of lower wheels
ϕ_1	rad	Direction angle of upper wheel
θ_p	rad	Pitch angle of pole
L_0	m	Length of pole (constant part)
L_1	m	Length of pole (variable part)
M_0	kg	Mass of lower wheels
M_1	kg	Mass of upper wheel
M_b	kg	Mass of ball screw

$$\boldsymbol{J}_{aco} = \begin{bmatrix} R & 0 & 0 & 0 \\ 0 & 1 & 0 & 0 \\ 0 & 0 & 1 & 0 \\ 0 & 0 & 0 & 1 \end{bmatrix} \cdots\cdots (5)$$

3.2 Dynamics of ITP The dynamics of the ITP is expressed as (6) derived from the Lagrange's equations.

$$\boldsymbol{M}(\boldsymbol{\theta})\ddot{\boldsymbol{\theta}} + \boldsymbol{H}(\boldsymbol{\theta}, \dot{\boldsymbol{\theta}}) + \boldsymbol{G}(\boldsymbol{\theta}) = \boldsymbol{T} \cdots\cdots (6)$$

Where, $\boldsymbol{M}(\boldsymbol{\theta})$ denotes the inertia matrix, $\boldsymbol{H}(\boldsymbol{\theta}, \dot{\boldsymbol{\theta}})$ denotes the centrifugal and Coriolis matrix, and $\boldsymbol{G}(\boldsymbol{\theta})$ denotes the gravity matrix.

3.3 Dynamics of Ball Screw The motion equations of the motor for the ball screw are expressed as (7) and (8).

$$J_b\ddot{\theta}_b = \tau_b^{mot} - \tau_b^{reac} - \tau_b^{dis} \cdots\cdots (7)$$

$$M_b\ddot{x}_b = F_b^{mot} - F_b^{reac} - F_b^{dis} \cdots\cdots (8)$$

Where, J_b, M_b are the inertial moment of the motor and inertia of the table, τ_b^{mot}, F_b^{mot} are the torque and force, τ_b^{reac}, F_b^{reac} are the reaction torque and reaction force that the motor receives from the ceiling, and τ_b^{dis}, F_b^{dis} are the disturbance torque and disturbance force added to the motor.

4. Walking Motion Estimation with IMU

In this section, how to estimate the human walking motion with an IMU is explained. One of the control purposes of this paper is to move the grasping point of the ITP at the same velocity with user's foot while walking as shown in Fig. 4. This movement refers to the walking pattern with a cane. In case of using a cane, the single ground point phase exists when the user moves the one side foot and the cane at the same time because it is necessary to lift up the cane to move it. On the other hand, in case of using the ITP, more than three ground points are kept at any time while walking because the ITP can move while stretching to the floor and ceiling at any time. Therefore, the movement of the ITP like Fig. 4 is effective, and the user of the ITP can walk more stably than using a cane. In this paper, the walking phase is defined, and the human walking motion is divided into the swing phase and stance phase as shown in Fig. 4. At the swing phase, the ITP moves together with user's foot synchronously. And at the stance phase, the ITP does not move. During the walking, the IMU sends the horizontal foot acceleration to the controller in real time.

4.1 Foot Motion Measurement Assuming the x-axis is the movement direction and y-axis is the orientation direction of walking, the horizontal foot acceleration $\alpha_{horizon}^{foot}$ is expressed as (9).

$$\alpha_{horizon}^{foot} = \alpha_x^{foot}\cos\theta_y^{foot} + \alpha_z^{foot}\sin\theta_y^{foot} \cdots\cdots (9)$$

Where, α_x^{foot} and α_z^{foot} represent the measurement acceleration of the x-axis and z-axis respectively, and θ_y^{foot} is the pitch angle of the foot. The pitch angle θ_y^{foot} is obtained as (10).

$$\theta_y^{foot}(t) = \int_0^t \dot{\theta}_y^{foot}(t)dt + \theta_{init}^{foot} \cdots\cdots (10)$$

Where, θ_{init}^{foot} is the initial pitch angle of the foot. Also, the horizontal foot velocity is expressed as (11) [9].

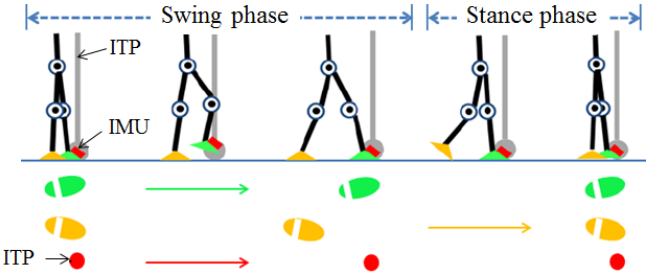

Fig. 4. Walking phase and ITP movement

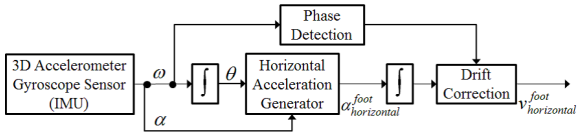

Fig. 5. Sensor data process diagram

$$v_{horizon}^{foot}(t) = \int_0^t \alpha_{horizon}^{foot}(t)dt, \qquad (t \in [0, T]) \cdots\cdots (11)$$

4.2 Walking Phase Detection The data received from the IMU must have the drift error during the integration. The drift error leads to the undesired control response in case of using the sensor data for the control. To reduce the drift error effect, the walking phase is used and the value initialization is applied at the stance phase. In this paper, the pitch angular velocity $\dot{\theta}_y^{foot}$ is used to detect the walking phase; the swing phase is defined by $\dot{\theta}_y^{foot} \neq 0$ or $\dot{\theta}_y^{foot}(t) - \dot{\theta}_y^{foot}(t-L)$ is large, and the stance phase is defined by $\dot{\theta}_y^{foot} \simeq 0$ and $\dot{\theta}_y^{foot}(t) - \dot{\theta}_y^{foot}(t-L)$ is small. L denotes the sampling time. Figure 5 shows the data process from the IMU to the controller.

5. Control System

In this section, the control system with the ITP is explained. First, the Reaction Torque Observer (RTOB) [10] are introduced. Second, the force control applied to the ball screw is introduced. Third, the mode decoupling method [12] applied to the lower and upper wheel of the ITP is explained. Fourth, the translation mode to control the position of the grasping point is explained. Fifth, the inclination mode to control the inclination of the ITP is also explained. And finally, the block diagram of the wheel part is described.

5.1 Reaction Torque Observer (RTOB) The Reaction Torque Observer (RTOB) estimates the reaction torque added to the upper wheel and ball screw. The motion equation including the disturbance is shown as (12).

$$\boldsymbol{M}\ddot{\boldsymbol{\theta}} = \boldsymbol{T}^{ref} - \left(\boldsymbol{T}^{fric} + \boldsymbol{T}^{dis}\right) \cdots\cdots (12)$$

The disturbance torque is compensated by using the Disturbance Observer (DOB) [11]. The disturbance torque caused by the friction torque $\boldsymbol{T}^{fric}$ is defined as (13).

$$\boldsymbol{T}^{fric} = \boldsymbol{F} + \boldsymbol{D}\dot{\boldsymbol{\theta}} \cdots\cdots (13)$$

Where, $\boldsymbol{F}$ is the coefficient of the static friction and $\boldsymbol{D}$ is the coefficient of the dynamic friction. The reaction torque $\hat{\boldsymbol{T}}^{reac}$ without $\boldsymbol{T}^{fric}$ can be estimated as (14).

$$\hat{\boldsymbol{T}}^{reac} = \boldsymbol{T}^{ref} - \boldsymbol{M}\ddot{\boldsymbol{\theta}} - \boldsymbol{T}^{fric} \cdots\cdots (14)$$

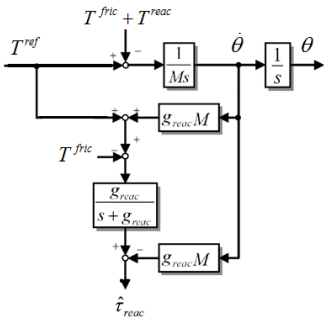

Fig. 6. Reaction torque observer (RTOB)

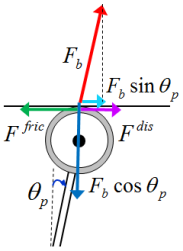

Fig. 7. Force relation between upper wheel and ceiling

(14) can be transformed as (15) by using the pseudo differentiator.

$$\hat{\boldsymbol{T}}^{reac} = \frac{g_{reac}}{s+g_{reac}}\left(\boldsymbol{T}^{ref} + g_{reac}\boldsymbol{M}\dot{\boldsymbol{\theta}} - \boldsymbol{T}^{fric}\right) - g_{reac}\boldsymbol{M}\dot{\boldsymbol{\theta}} \quad \cdots\cdots (15)$$

In the equation, s is the laplace operator and g_{reac} is the cut off frequency for the pseudo differentiator. The block diagram of the RTOB is shown as Fig. 6.

5.2 Force Control The force control applied to the ball screw is expressed as (16).

$$F_b^{ref} = K_b^{ball}\left(F_b^{cmd} - \tilde{F}_b^{reac}\right) \cdots\cdots (16)$$

Where, K_b^{ball} is the force gain, and $\tilde{F}_b^{reac}$ is the estimated reaction force provided by the RTOB. The desired tension force between the floor and ceiling is generated by using the force control.

In this study, it is intended that the upper and lower ends of the ITP do not slip and the ITP does not fall down by the external force. Therefore, it is necessary to generate the force command which prevents the slip of the ends of the ITP. In this paper, the slip between the upper wheel and the ceiling is focused on. The force relation between the upper wheel and the ceiling during the control is shown in Fig. 7.

Where, F_b is the tension force provided by the ball screw, F^{dis} is the external force, and F^{fric} is the friction force. The condition to prevent the slip between the upper wheel and the ceiling is obtained as (17).

$$\mu N \geq \left|F^{dis} + F_b \sin\theta_p\right| \cdots\cdots (17)$$

Where, μ is the static friction coefficient, and N is the vertical drag. Because the vertical drag N is provided by the tension force, (17) is rewritten as (18), and (19) is obtained.

$$\mu F_b \cos\theta_p \geq \left|F^{dis} + F_b \sin\theta_p\right| \cdots\cdots (18)$$

$$F_b \geq \frac{\left|F^{dis} + F_b \sin\theta_p\right|}{\mu \cos\theta_p} \cdots\cdots (19)$$

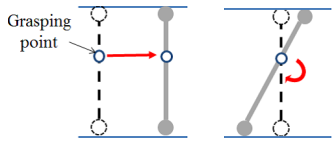

(a) Translation mode (b) Inclination mode

Fig. 8. Images of mode

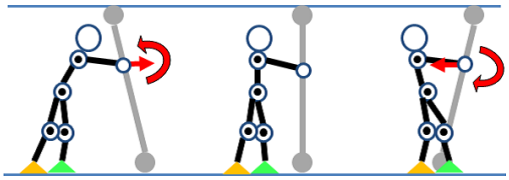

Fig. 9. Image of inclination control

Then, F^{dis} and $F_b \sin\theta_p$ can be estimated by the RTOB of the upper wheel as $\tilde{F}_{w1}^{reac}$. Consequently, it is able to prevent the slip between the upper wheel and the ceiling by generating the force command as (20).

$$F_b^{cmd} = \frac{\left|\tilde{F}_{w1}^{reac}\right|}{\mu \cos\theta_p} + \alpha \cdots\cdots (20)$$

Where, α denotes the margin force to prevent the slip, so it must be the arbitrary positive constant number.

5.3 Mode Decoupling Method In this paper, the mode decoupling method is applied to the lower and upper wheel of the ITP in order to independently control the position of the grasping point to the front-back direction (translation mode) and the inclination of the ITP (inclination mode). The images of the translation mode and inclination mode are shown in Fig. 8(a) and Fig. 8(b).

In case of using the ITP, the most dangerous factor is the falling down by the external force and slip of ground point. In addition to the force control of the ball screw, by applying the inclination control of the ITP, the risk of falling down of the ITP can be reduced. When the external force is added, the risk of falling down can be reduced by inclining the ITP to the opposite direction against the external force. The image of the inclination control is shown in Fig. 9. However, the inclination change of the ITP influences the position of the grasping point to the front-back direction, which can cause the reduction of user comfort. Therefore, it is necessary to control both the position of the grasping point and the inclination of the ITP independently in order to track both of the desired position of the grasping point and the desired inclination of the ITP.

The mode matrix can transform each physical parameter of the systems into the virtual modal parameters. In this paper, the second-order mode matrix $\boldsymbol{Q}_2$ is defined as (21)

$$\boldsymbol{Q}_2 = \frac{1}{L_a + L_b}\begin{bmatrix} L_a & L_b \\ -1 & 1 \end{bmatrix} \cdots\cdots (21)$$

Where, L_a and L_b are the length from the grasping point to the ground point of the ITP at the ceiling and floor respectively. Each position of the grasping point and the inclination of the ITP is transformed into the modal space as (22) by using the second-order mode matrix $\boldsymbol{Q}_2$.

$$\begin{bmatrix} x_g \\ x_\theta \end{bmatrix} = \boldsymbol{Q}_2 \begin{bmatrix} R\phi_0 \\ r\phi_1 \end{bmatrix} \cdots\cdots (22)$$

Where, x_g and x_θ are the translational position of the grasping point and the inclination of the ITP respectively. The modal acceleration references $\ddot{x}_g^{ref}$ and $\ddot{x}_\theta^{ref}$ are realized and distributed into each lower and upper wheel by using the inverse mode matrix as shown in (23).

$$\begin{bmatrix} R\ddot{\phi}_0^{ref} \\ r\ddot{\phi}_1^{ref} \end{bmatrix} = \boldsymbol{Q}_2^{-1} \begin{bmatrix} \ddot{x}_g^{ref} \\ \ddot{x}_\theta^{ref} \end{bmatrix} \cdots\cdots (23)$$

5.4 Translation Mode In the translation mode, the virtual impedance command generator and the P control are applied to the position of the grasping point control in modal space. The P control enables the grasping point of the ITP to move same velocity as the user's foot. However, in case of applying the only P control, the big acceleration change of the ITP is produced, especially at the start and end of step. It is not so good for user in terms of the user comfort. In order to suppress the big acceleration change, the virtual impedance command generator using the virtual force is applied. At first, the virtual force is expressed as (24).

$$F_c = D_v v_{horizon}^{foot} \cdots\cdots (24)$$

Where, F_c is the virtual force command, and D_v is the virtual viscosity coefficient. Then, the virtual impedance command is designed as (25).

$$M_c \alpha_c^{cmd} + D_c v_c^{cmd} = F_c \cdots\cdots (25)$$

Where, M_c and D_c denote the virtual mass and virtual damper, α_c^{cmd} and v_c^{cmd} denote the acceleration and velocity command to the grasping point in modal space. The acceleration reference is expressed as (26).

$$\ddot{x}_g^{ref} = K_v^g \left(v_c^{cmd} - \dot{x}_g^{res} \right) + \alpha_c^{cmd} \cdots\cdots (26)$$

Where, K_v^g is the velocity gain. Accordingly, the lower and upper wheel rotate so that the position of the grasping point tracks the human foot speed while suppressing the acceleration change by the virtual impedance command generator and P control.

5.5 Inclination Mode In the inclination mode, the PD control applied to the inclination control of the ITP in modal space is expressed as (27).

$$\ddot{x}_\theta^{ref} = K_p^\theta \left(x_\theta^{cmd} - x_\theta^{res} \right) + K_v^\theta \left(\dot{x}_\theta^{cmd} - \dot{x}_\theta^{res} \right) \cdots\cdots (27)$$

Where, K_p^θ is the position gain and K_v^θ is the velocity gain. The lower and upper wheel rotate so that the desired inclination is realized quickly by the PD control. The command of the inclination x_θ^{cmd} is defined by the stability of the system including the human and ITP. To consider the stability of the system, the Zero-moment point (ZMP) and Center of gravity (COG) is applied.

The ZMP is a point on the ground where the total moment generated by the gravity and inertia becomes to zero as shown in (28).

$$x_{ZMP} = \frac{\sum_i^n m_i x_i (\ddot{z}_i + g) - \sum_i^n m_i \ddot{x}_i z_i - \sum_i^n I_{iy} \ddot{\theta}_{iy}}{\sum_i^n m_i (\ddot{z}_i + g)} \cdots\cdots (28)$$

Where, m_i is the mass of the robot or human, x_i, y_i, z_i are the positions of the center of mass in each body, I_i is the inertia component, and $\ddot{\theta}_i$ are the angular acceleration. When the floor reaction force can be measured, the ZMP is obtained as (29).

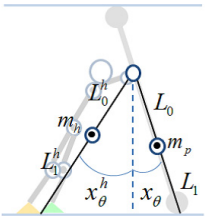

Fig. 10. System model of human and ITP

$$x_{ZMP} = \frac{\sum_i^n f_i x_{zi}}{\sum_i^n f_i} \cdots\cdots (29)$$

Where, x_{zi} is the position of the ground point, and f_i is the measured floor reaction force. The ZMP is also known as the center of pressure. Also, the COG position is defined as (30).

$$x_{COG} = \frac{\sum_i m_i x_{ci}}{\sum_i m_i} \cdots\cdots (30)$$

Where, x_{ci} is the position of the center of mass in each body. In this research, the system of the human and ITP is modeled as the two rigid bodies leaning against each other as shown in Fig. 10.

Where, m_h and m_p are the mass of the human and ITP, L_0^h and L_1^h are the length from the center of mass of the human to the grasping point and to the ground point of the human at floor, L_0 and L_1 are the length from the center of mass of the ITP to the grasping point and to the ground point of the ITP at floor, and x_θ^h and x_θ are the inclination of the human and ITP, respectively. Then, the ZMP position is derived from (31).

$$x_{ZMP} = \frac{m_p (L_0 + L_1) \sin(x_\theta) + m_h \left(L_0^h + L_1^h \right) \sin\left(-x_\theta^h \right)}{m_p + m_h} \cdots\cdots (31)$$

Also, the COG position is derived from (32).

$$x_{COG} = \frac{m_p L_0 \sin(x_\theta) + m_h L_0^h \sin\left(-x_\theta^h \right)}{m_p + m_h} \cdots\cdots (32)$$

The most stable condition of this system is expressed as (33).

$$x_{ZMP} = x_{COG} \cdots\cdots (33)$$

Therefore, the command of the inclination x_θ^{cmd} is derived from (34)

$$x_\theta^{cmd} = \sin^{-1} \left(\frac{L_1^h m_h}{L_1 m_p} \sin\left(x_\theta^h \right) \right) \cdots\cdots (34)$$

However, the inclination of the human x_θ^h can't be measured because no sensor to measure the inclination of the human is attached. Then, the estimated reaction torque of the upper wheel is usable to estimate the inclination of the human. Figure 11 shows the system model and the external force from the human.

Where, F_0^h and F_1^h are the external force from the human

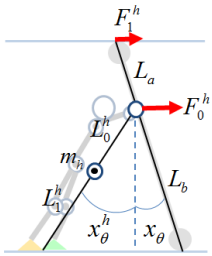

Fig. 11. System model and external force from human

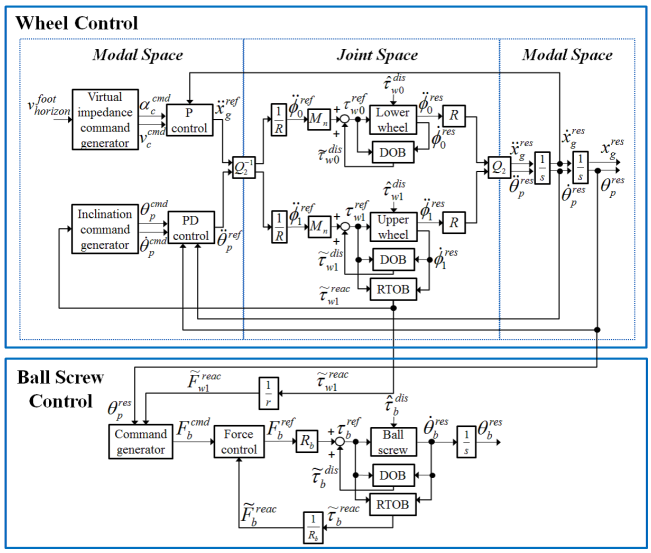

Fig. 12. Block diagram of whole system

added to the grasping point and the upper wheel. The moment balance of the human is derived from (35).

$$m_h g L_1^h \sin\left(x_\theta^h\right) = F_0^h \left(L_0^h + L_1^h\right) \cos\left(x_\theta^h\right) \cdots\cdots\cdots (35)$$

Then, F_0^h is obtained as (36) by rewriting (35).

$$F_0^h = \frac{L_1^h}{L_0^h + L_1^h} m_h g \tan\left(x_\theta^h\right) \cdots\cdots\cdots\cdots\cdots\cdots (36)$$

In addition, F_1^h is derived from (37).

$$F_1^h = \frac{L_b}{L_a + L_b} F_0^h \cdots\cdots\cdots\cdots\cdots\cdots\cdots\cdots (37)$$

Therefore, the estimated reaction torque of the upper wheel $\tilde{\tau}_{w1}^{reac}$ is expressed as (38).

$$\tilde{\tau}_{w1}^{reac} = \frac{r L_b L_1^h}{(L_a + L_b)\left(L_0^h + L_1^h\right)} m_h g \tan\left(x_\theta^h\right) \cdots\cdots\cdots (38)$$

As a result, the inclination of the human x_θ^h can be derived from the estimated reaction torque of the upper wheel $\tilde{\tau}_{w1}^{reac}$ as (39).

$$x_\theta^h = \tan^{-1}\left(\frac{\tilde{\tau}_{w1}^{reac}(L_a + L_b)(L_0^h + L_1^h)}{r L_b L_1^h m_p g}\right) \cdots\cdots\cdots (39)$$

5.6 Block Diagram The block diagram of the whole system is shown as Fig. 12. In this system, the force control is applied to the ball screw, and the mode decoupling method is applied to the wheel part. In modal space, the virtual impedance command generator and P control are applied to the control of the position of the grasping point, and the PD control is applied to the control of the inclination of the ITP. The control objects x_g and x_θ in modal space are transformed into the joint space by the inverse mode matrix $\boldsymbol{Q}_2^{-1}$, and these responses are obtained by the mode matrix $\boldsymbol{Q}_2$.

Table 2. Experimental parameters

Parameter	Value	Name
K_v^g	70.0	Velocity gain of lower wheels
K_p^θ	400.0	Position gain of upper wheel
K_v^θ	40.0	Velocity gain of upper wheel
M_c	30.0	Virtual mass of compliance control
D_c	100.0	Virtual damper of compliance control
D_v	100.0	Virtual damper of compliance control
K_b^{ball}	4.0	Force gain of ball screw
g^{w0}	50.0	Cut off frequency of DOB of lower wheels
g^{w1}	50.0	Cut off frequency of DOB of upper wheel
g^{ball}	50.0	Cut off frequency of DOB of ball screw
g_{reac}^{w1}	50.0	Cut off frequency of RTOB of upper wheel
g_{reac}^{ball}	50.0	Cut off frequency of RTOB of ball screw
α	20	Margin force
μ	0.7	Static friction coefficient（assumption）
L_a	1.12	ITP length from grasping point to ceiling
L_b	1.45	ITP length from grasping point to floor
L_0	0.85	ITP length from COG to grasping point
L_1	0.60	ITP length from COG to floor
L_0^h	0.60	Human length from COG to grasping point
L_1^h	1.00	Human length from COG to floor
m_p	44.0	Mass of ITP
m_h	76.0	Mass of human

6. Experiment

The effectiveness of the proposed control system is evaluated through two experiments.

6.1 Experiment Condition The parameters used in the experiments are shown in Table 2.

6.1.1 Condition of Experiment 1 The translation mode is tested. The position of the grasping point is controlled to move together with user's foot synchronously. Then, the command of the inclination is set as $x_\theta^{cmd} = 0$. The walking data of four forward steps received from the IMU is input to the robot control in real time. The output of the proposed control by the virtual impedance command generator and P control is compared with the output without the proposed it, in terms of the user comfort by using the index of the ISO 5349-1 [13]. It is derived by the acceleration response as shown in (40).

$$a_t = \left[\sum_{i=1}^{n} (W_i a_i)^2\right]^{\frac{1}{2}} \cdots\cdots\cdots\cdots\cdots\cdots\cdots (40)$$

Where, a_t is the frequency-weighted acceleration, a_i is the acceleration in one-third octave band in each frequency, and W_i is the weighting factor. So, the acceleration, the moving distance of the grasping point, and the result of the ISO 5349-1 are observed in the experiment 1.

6.1.2 Condition of Experiment 2 The inclination mode is tested. The external force from the human is added to the ITP. Then, the command of the translation is set as $x_g^{cmd} = 0$, and the threshold is set as $x_\theta^{cmd} = 0$ for $|\tilde{\tau}_{w1}^{reac}| < 0.1$. The estimated reaction torque of the upper wheel, the inclination response, and the stability from the positions of the ZMP and COG are observed in the experiment 2.

6.2 Experiment Result The results of the experiment

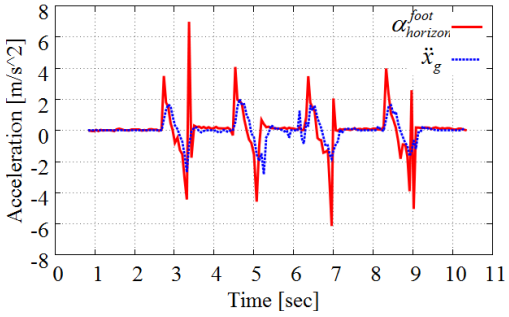

Fig. 13. Acceleration of foot and grasping point

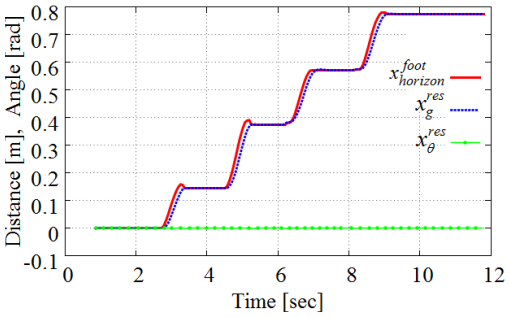

Fig. 14. Moving distance of foot and grasping point

Table 3. Index of ISO 5349-1

Method	Average of $a_t[m/s^2]$
Without Proposed Control	0.054
With Proposed Control	0.028

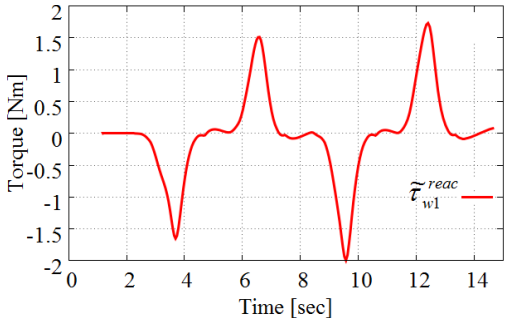

Fig. 15. Estimated reaction torque of upper wheel

1 and the experiment 2 are shown and explained.

6.2.1 Result of Experiment 1 Figure 13 shows the horizontal acceleration of the foot received from the IMU and the grasping point. Thanks to the virtual impedance command generator, the acceleration change is suppressed. Figure 14 shows the moving distance of the foot received from the IMU and the grasping point, and the inclination response of the ITP. Due to the application of the virtual impedance command generator, the position response has a little delay, but the undesired moving is prevented. Moreover, thanks to the mode decoupling method, the desired inclination response is obtained regardless of the translational moving. In addition, Table 3 shows the results of the ISO 5349-1 whose values are the average of four times four forward steps. From the result, the user comfort is improved by the proposed control.

6.2.2 Result of Experiment 2 Figure 15 shows the estimated reaction torque of the upper wheel, and Fig. 16

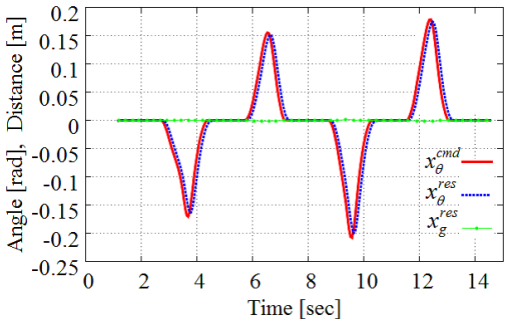

Fig. 16. Inclination response of ITP

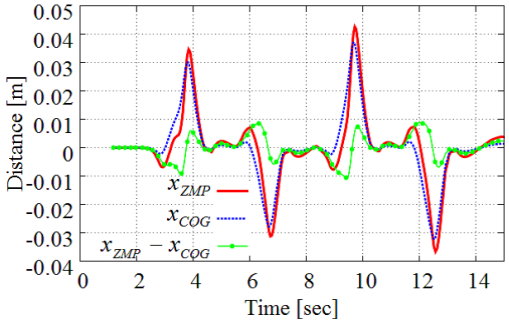

Fig. 17. Position of ZMP and COG

shows the inclination command and response of the ITP, and the translation response of the grasping point. The inclination control is conducted accurately according to the estimated reaction torque of the upper wheel. Moreover, thanks to the mode decoupling method, the desired translation response of the grasping point is obtained regardless of the inclination of the ITP. In addition, Fig. 17 shows the positions of the ZMP and COG, and the difference between these positions. From the result, the difference between the positions of the ZMP and COG is suppressed. Therefore, the inclination control which maintain the stability of the system including the human and ITP is realized. As a result, it is expected that the risk of falling down of the ITP is reduced.

7. Conclusion

In this paper, the structure and control system of a novel assist device, Intelligent Tension Pole (ITP), to assist walking, standing up and sitting down in indoor are proposed. There are few devices which focus on assisting all of three motions without inconvenience by size or stability, though many kinds of the motion assist device are developed. Therefore, the ITP is proposed which is expected to provide support for achieving self-reliance, space saving, and stability. Wheels are added to the lower and upper ends of the tension pole. In addition, the ball screw which enables the ITP to move while stretching to the floor and ceiling at any time by the force control is added. In order to improve user comfort and reduce the risk of falling down of the ITP, the translation control and inclination control of the ITP are applied to the wheel control. These controls are controlled independently by the mode decoupling method. The validity of the proposed control system was tested through experiments. The translation mode and inclination mode control was conducted independently according to the movement of the IMU attached on the foot and the estimated reaction torque of the upper wheel

respectively. Thanks to the proposed method, the acceleration change and undesired moving are suppressed. Therefore, the user comfort is improved. In addition, the stability of the system including the human and ITP is maintained regardless of the external force from the human. As a result, it is expected that the risk of falling down of the ITP is reduced.

Acknowledgment

This work was supported in part by a Grant-in-Aid for Scientific Research (15H02235).

References

(1) Y. Wang and S. Wang: "Motion Control of a Walking Support Robot Considering Pressure and Thrust from Users", Soft Computing and Intelligent Systems (SCIS), 2014 Joint 7th International Conference on and Advanced Intelligent Systems (ISIS), 15th International Symposium, pp.392–937 (2014)
(2) R. Tan, S. Wang, Y. Jiang, K. Ishida, and M. Nagano: "Adaptive Controller for Motion Control of an Omni-directional Walker", Mechatronics and Automation (ICMA), 2010 International Conference, pp.156–161 (2010)
(3) M. Sasayama and T. Murakami: "Realization of gait rehabilitation using compliant force coordinate transformation control", IECON 2013, 39th Annual Conference of the IEEE Industrial Electronics, pp.3982–3987 (2013)
(4) R. Kamnik and T. Bajd: "Robot Assisted Standing-up", IRobotics and Automation, 2000. Proceedings. ICRA '00. IEEE International Conference, Vol.3, pp.2907–2912 (2000)
(5) T. Hatsukari, S. Kuroko, N. Miyake, J. Higuchi, R. Kawazoe, Y. Hirata, and K. Kosuge: "Self-help Standing-up Method Based on Quasi-static Motion", Robotics and Biomimetics, 2008. ROBIO 2008. IEEE International Conference, pp.342–347 (2009)
(6) E. Strickland: "Good-bye, Wheelchair", IEEE Spectrum, pp.24–26 (2012)
(7) H. Kawamoto, T. Hayashi, T. Sakurai, K. Eguchi, and Y. Sankai: "Development of Single Leg Version of HAL for Hemiplegia", 31st Annual International Conference of the IEEE EMBS, pp.5038–5043 (2009)
(8) R. Hanaoka, T. Nozaki, and T. Murakami: "Cooperation Control of ITP with Human Based Inertial Measurement Unit", IECON 2016, 42nd Annual Conference of the IEEE Industrial Electronics Society, Proceedings (2016)
(9) C. Yang and T. Murakami: "Novel Walking Assist Device Based on Mobile Manipulator and Inertial Measurement Unit", *IEEJ Journal of Industry Applications*, Vol.3, No.5, pp.381–387 (2014)
(10) T. Murakami, F. Yu, and K. Ohnishi: "Torque Sensorless Control in Multidegree-of-Freedom Manipulator", *IEEE Transactions on Industrial Electronics*, Vol.40, No.2, pp.259–265 (1993)
(11) K. Ohnishi, M. Shibata, and T. Murakami: "Motion Control for Advanced Mechatronics", *IEEE/ASME Transactions on Mechatronics*, Vol.1, No.1, pp.56–67 (1996)
(12) S. Katsura and K. Ohnishi: "Modal System Design of Multirobot Systems by Interection Mode Control", *IEEE Transactions on Industrial Electronics*, Vol.54, No.3, pp.1537–1546 (2007)
(13) International Organization for Standardaization: "Mechanical vibration—Measurement and evaluation of human exposure to hand-transmitted vibration—Part 1: General requirements", ISO 5349-1 (2001)

Ryo Hanaoka (Non-member) received the B.E. degrees from Keio University, Yokohama, Japan, in 2015. He is currently a graduate student in Keio University.

Takahiro Nozaki (Member) received the B.E. degree in system design engineering and the M.E. and Ph.D. degrees in integrated design engineering from Keio University, Yokohama, Japan, in 2010, 2012, and 2014, respectively. After working at Yokohama National University, Yokohama, Japan, as an Assistant Professor for one year, he joined Keio University as an Assistant Professor in 2015.

Toshiyuki Murakami (Fellow) received the B.E., M.E., and Ph.D. degrees in electrical engineering from Keio University, Yokohama, Japan, in 1988, 1990, and 1993, respectively. In 1993, he joined the Department of Electrical Engineering, Keio University, where he is currently a Professor in the Department of System Design Engineering. From 1999 to 2000, he was a Visiting Researcher with The Institute for Power Electronics and Electrical Drives, Aachen University of Technology, Aachen, Germany. His research interests are robotics, intelligent vehicles, mobile robots, and motion control.